Improving Spectral Responsivity Measurements by Correcting for Filter Bandwidth

Clara Edmonds and Harald Müllejans

***Abstract*—Spectral responsivity (SR) measurements are key in characterizing photovoltaic (PV) devices and calculating spectral mismatch correction factors (MMF). SR is measured using different wavelengths of monochromatic light. In practical measurement systems, this light has a finite bandwidth, meaning that it is only quasi-monochromatic. The data analysis, however, typically assumes perfectly monochromatic light. The accuracy of the calculated SR then depends not only on the actual bandwidth of the monochromatic light used during the measurement but also on the intensity distribution inside the bandwidth. In our SR measurement system, we use quasi-monochromatic light obtained from a solar simulator and a range of bandpass filters. First, we measured and analyzed the spectral content of light transmitted for each filter. Then, we developed an iterative correction scheme for the measured SR. This numerical approach assumes no previous knowledge about the SR of the device under test (DUT). Applying this scheme for bandwidth correction to a range of PV cells with varying SR curves, we found that the corrections for most wavelengths are of minor importance. However, for those wavelengths where the shape of the SR curve of the reference device and DUT differ notably, the corrections are significant up to 20% and higher. We investigated the change in the spectral MMF, which was found to be negligible in most cases but not always. Therefore, the bandwidth correction is mainly important not only for improving SR measurements of PV devices but also relevant for the determination of spectral mismatch factors.**

***Index Terms*—Photovoltaic (PV) device measurements, spectral responsivity (SR).**

I. Introduction

SPECTRAL responsivity (SR) of photovoltaic (PV) devices [1] is a key parameter for the characterization of their electrical performance [2]. While the performance itself is measured using natural or simulated sunlight, it has to be reported at so-called standard test conditions with a defined spectral content of sunlight [3]. The simulated sunlight used during electrical performance measurement in practice, however, will always differ from this defined spectral irradiance [3]. This means a spectral mismatch error [4] is made during the measurement and has to be corrected using the SR of the PV device under test (DUT) [1] [2].

The SR of a PV device at a given wavelength can be determined by illuminating the device with monochromatic light of that wavelength and comparing its measured electrical output to the output of a calibrated reference device. Using monochromatic light of varying wavelengths, the SR of the DUT can be determined over the wavelength range of interest. Measurement systems for SR use different ways of obtaining the monochromatic light. The most common ones are monochromators using diffraction gratings [5], filter-based systems using bandpass filters [6], [7], and more recently LED light sources [8], [9], [10]. The use of tunable lasers has also been reported [11]. In all these systems, the light is not perfectly monochromatic, but rather quasi-monochromatic as there is a finite bandwidth of the monochromatic light. A larger bandwidth of quasi-monochromatic light is less costly in terms of instrumentation, yields larger measurement signals, and has a higher signal-to-noise ratio. However, it also leads to the loss of spectral resolution in the measured SR. The data analysis required to calculate the SR of the DUT assumes perfectly monochromatic light and does not account for this loss of spectral resolution.

Correction schemes for the bandwidth of the monochromatic light in the measurement of SR have been proposed before and implemented [8], [9], [10], including a correction for spectroradiometer bandwidth [12]. However, they are not readily applicable to filter-based systems. For example, the method in [12] requires equispaced data points, which are generally not available on filter-based systems.

An iterative solution has been outlined for an LED-based system [10]. While this scheme contains the main elements required, its simple description did not consider the practical implications when implementing it for a filter-based system. Here, we apply such a scheme for the first time to a filter-based system, which presents different challenges and requires additional considerations in measurements and data analysis.

We investigate the effect of the bandwidth of our filter-based SR measurement system [7] on the accuracy of the determined SR. First, we characterize each filter with the spectral content of the transmitted light. Then, we present a numerical correction scheme for the calculation of the SR using an iterative procedure. This is applied to the SR data measured for four typical PV cells, representing a range of different SR shapes. The improvement in accuracy of the SR and effect on the spectral mismatch correction factor (MMF) is evaluated.

Manuscript received 22 September 2022; revised 8 November 2022; accepted 3 December 2022. Date of publication 23 December 2022; date of current version 12 January 2023. *(Corresponding author: Harald Müllejans.)*

The authors are with European Commission, Joint Research Centre (JRC), 21027 Ispra (VA), Italy (e-mail: claraaskgaard@gmail.com; harald.muellejans@ec.europa.eu).

Color versions of one or more figures in this article are available at https://doi.org/10.1109/JPHOTOV.2022.3228103.

Digital Object Identifier 10.1109/JPHOTOV.2022.3228103

II. Methods

In this section, we will first summarize the theory of SR measurement and then propose an iterative scheme to improve the data analysis. In the last part, we present the SR measurement system.

According to IEC 60904-8 [1], there are two methods for determining the SR of a PV device. The first consists of irradiating the DUT with a narrow-bandwidth light source at a series of different wavelengths covering its responsivity range, and measuring short-circuit current and monochromatic irradiance at each of these wavelengths. This method results in the spectral irradiance responsivity with the unit A/(W/m^2). To determine the SR, this needs to be divided by the active area of the DUT. For the second method, the short-circuit current and monochromatic light beam *power* are measured. This directly yields the SR (also called spectral power responsivity) in the unit of A/W. Here, we use exclusively the second method: SR for spectral (power) responsivity.

A. Theory of Spectral Responsivity Measurement

The short-circuit current I generated in a PV device and the spectral responsivity $\mathrm{SR}(\lambda)$ are related by

$$I = A \int E(\lambda)\,\mathrm{SR}(\lambda)\,d\lambda \tag{1}$$

where λ is the wavelength, A is the active area of the device, and $E(\lambda)$ is the spectral irradiance [1]. The currents for each filter n for the DUT and reference device (REF) are, therefore

$$I_{\mathrm{REF},n} = A_{\mathrm{REF}} \int E_n(\lambda)\,\mathrm{SR}_{\mathrm{REF}}(\lambda)\,d\lambda \tag{2}$$

$$I_{\mathrm{DUT},n} = A_{\mathrm{DUT}} \int E_n(\lambda)\,\mathrm{SR}_{\mathrm{DUT}}(\lambda)\,d\lambda \tag{3}$$

where $E_n(\lambda)$ is the irradiance transmitted through filter n, with $n = 1, 2, 3, \ldots, N$ and N the total number of filters (i.e., distinct wavelengths) in the measurement data. Dividing (3) by (2) and rearranging gives

$$\int E_n(\lambda)\,\mathrm{SR}_{\mathrm{DUT}}(\lambda)\,d\lambda = \frac{A_{\mathrm{REF}}}{A_{\mathrm{DUT}}}\frac{I_{\mathrm{DUT}}}{I_{\mathrm{REF}}}\bigg|_n \int E_n(\lambda)\,\mathrm{SR}_{\mathrm{REF}}(\lambda)\,d\lambda. \tag{4}$$

Note that the SRs for the devices are continuous functions and identical for all filters *n*. Equation (4) is often simplified, neglecting the spectral distribution of the quasi-monochromatic light and assuming perfectly monochromatic light to

$$\mathrm{SR}_{\mathrm{DUT}}(\lambda_n) = \frac{A_{\mathrm{REF}}}{A_{\mathrm{DUT}}}\frac{I_{\mathrm{DUT}}}{I_{\mathrm{REF}}}\bigg|_n \mathrm{SR}_{\mathrm{REF}}(\lambda_n) \tag{5}$$

so that the SR of DUT at the wavelength λ_n of filter n is equal to the SR of the REF at the same wavelength multiplied by the ratio of the measured currents and the ratio of device active areas. In an experimental setup, $\mathrm{SR}_{\mathrm{DUT}}(\lambda)$ can, therefore, be determined by illuminating the DUT as well as a REF with known $\mathrm{SR}_{\mathrm{REF}}(\lambda)$ with monochromatic light of successively different wavelengths and measuring the currents generated in the two devices.

B. Iterative Correction Scheme

In this work, we want to improve the data analysis of the SR measurement and use (4) rather than the simplified version (5). All the parameters on the right-hand side of (4) are known or can be measured. On the left-hand side, we have two unknowns, $\mathrm{SR}_{\mathrm{DUT}}(\lambda)$ and $E_n(\lambda)$, which can be determined by measurement (see section III A). However, it is not possible to determine analytically $\mathrm{SR}_{\mathrm{DUT}}(\lambda)$ due to the integral.

The SR measurement uses N filters; therefore, we have N data points at different wavelengths. We propose to use an iterative numerical scheme to determine $\mathrm{SR}_{\mathrm{DUT}}(\lambda)$, starting only from the experimental data available and making no assumptions about the SR of the DUT.

In the following, we will use the iteration index i starting from 0, 1, 2, …

Assuming we would have an estimate of $\mathrm{SR}_{\mathrm{DUT},i}(\lambda)$, we aim to improve this estimate by applying a correction factor. If (4) is rearranged to

$$\frac{A_{\mathrm{REF}}}{A_{\mathrm{DUT}}}\frac{I_{\mathrm{DUT}}}{I_{\mathrm{REF}}}\bigg|_n \frac{\int E_n(\lambda)\,\mathrm{SR}_{\mathrm{REF}}(\lambda)\,d\lambda}{\int E_n(\lambda)\,\mathrm{SR}_{\mathrm{DUT},i}(\lambda)\,d\lambda} = 1 \tag{6}$$

the left-hand side can be evaluated and, for consistency, should equal unity. However, in general, this will not be the case but rather give a numerical value $c_i(\lambda_n)$ for each filter

$$\frac{A_{\mathrm{REF}}}{A_{\mathrm{DUT}}}\frac{I_{\mathrm{DUT}}}{I_{\mathrm{REF}}}\bigg|_n \frac{\int E_n(\lambda)\,\mathrm{SR}_{\mathrm{REF}}(\lambda)\,d\lambda}{\int E_n(\lambda)\,\mathrm{SR}_{\mathrm{DUT},i}(\lambda)\,d\lambda} = c_i(\lambda_n). \tag{7}$$

Most variables on the left-hand side are given and fixed in the sense that they do not change with iteration i. The only quantity that can be varied is $\mathrm{SR}_{\mathrm{DUT},i}(\lambda)$.

We can now improve the estimate $\mathrm{SR}_{\mathrm{DUT},i}(\lambda)$ in (6) by multiplying it with $c_i(\lambda_n)$ such that

$$\mathrm{SR}_{\mathrm{DUT},i+1}(\lambda_n) = c_i(\lambda_n) \cdot \mathrm{SR}_{\mathrm{DUT},i}(\lambda_n) \tag{8}$$

and, from (8), it is clear that $c_i(\lambda_n)$ is, therefore, the correction factor to improve in an iterative scheme the estimated SR of the DUT. The next iteration for the SR of the DUT according to (8) should improve such that the equality in (6) is reached. However, this will normally not be fully achieved, as the correction factor corrects $\mathrm{SR}_{\mathrm{DUT},i}(\lambda_n)$, i.e., one data point, whereas in (6) and (7), $\mathrm{SR}_{\mathrm{DUT},i}(\lambda)$ is used, i.e., all data points. The iterations must, thus, be continued until convergence is achieved, meaning that $c_i(\lambda_n) = 1$ for all N filters.

Using (2) and (3) and distinguishing between the current I measured in experiment from those calculated, we can rewrite (7) as follows:

$$c_i(\lambda_n) = \frac{I_{\mathrm{DUT}}}{I_{\mathrm{REF}}}\bigg|_{\mathrm{meas},n} \frac{I_{\mathrm{REF}}}{I_{\mathrm{DUT},\,i}}\bigg|_{\mathrm{calc},n} \tag{9}$$

with $c_i(\lambda_n)$ the correction factor for filter n on the i^{th} iteration. For each iteration, we have N correction factors.

At the start of the iteration, no previous knowledge of $\mathrm{SR}_{\mathrm{DUT}}$ is assumed, setting

$$\mathrm{SR}_{\mathrm{DUT},0}(\lambda) = 1 \tag{10}$$

for all wavelengths [10]. Then, using (7)

$$c_0(\lambda_n) = \frac{A_{\mathrm{REF}}}{A_{\mathrm{DUT}}}\frac{I_{\mathrm{DUT}}}{I_{\mathrm{REF}}}\bigg|_n \frac{\int E_n(\lambda)\,\mathrm{SR}_{\mathrm{REF}}(\lambda)\,d\lambda}{\int E_n(\lambda)\,d\lambda} \tag{11}$$

and with (8)

$$\mathrm{SR}_{\mathrm{DUT},1}\ (\lambda_n) = c_0\,(\lambda_n) \cdot \mathrm{SR}_{\mathrm{DUT},0}\ (\lambda_n) = c_0\,(\lambda_n)\,. \quad (12)$$

The first correction factor $c_0(\lambda_n)$ is, therefore, equal to the first estimate of SR, which sometimes is used rather than (5) [5]. It represents an improvement with respect to (5) as it considers explicitly the bandwidth of the transmitted light for the filters with respect to the REF. However, in order to consider this effect for the DUT, the iterative scheme has to be applied. We have implemented this scheme in MATLAB using piecewise Hermite polynomials for interpolation.

C. Spectral Responsivity Measurement System

The SRs of the PV cells were measured with a dedicated system at the European Solar Test Installation (ESTI) [7]. DUT and REF are placed next to each other and illuminated simultaneously with the same chopped monochromatic light (Xenon light source with 64 bandpass filters) as well as an additional continuous white bias light. The currents generated by the monochromatic light in the two PV devices are measured simultaneously using two lock-in amplifiers. The temperature of both devices is controlled to 25 °C by water and Peltier cooling, respectively.

III. Results and Discussion

In this section, we will first present the measurements of spectral irradiance transmitted by the filters of the SR measurement system, then the measurement of the SRs and their correction with the iterative scheme. Next, we investigate the convergence, possible refinements and a validation of the iterative scheme. Finally, the importance of SR bandwidth correction for spectral mismatch correction in the electrical performance measurement of PV devices will be investigated.

A. Measuring Spectral Irradiance Transmitted by Filters

To implement the iterative scheme, the spectral irradiance transmitted by each filter is required, as for example in (7) or (11). As a first step, the spectral irradiance of the light transmitted through each of the 64 filters of the ORIEL SR measurement system at ESTI [7] was measured with a fixed grating spectroradiometer (Instrument Systems CAS 140) (see Fig. 1).

The full-width half maxima range from 5 to 35 nm. Several transmission spectra revealed asymmetrical peaks or shoulders on either side of the peak wavelength (see Figs. 1 and 2). The wavelength λ_{cent} assigned to filter n is the centroid wavelength, where $E_n(\lambda)$ is the spectral irradiance measured for this filter [1], [2], [3]

$$\lambda_{\mathrm{cent},n} = \frac{\int \lambda \cdot E_n\,(\lambda)\,d\lambda}{\int E_n\,(\lambda)\,d\lambda}. \quad (13)$$

The measured transmitted irradiance was consistent with that calculated from the lamp spectrum and the separately measured filter transmission curves (not shown). To minimize the influence of noise, the spectral irradiance data were cut off below 1% level of the peak irradiance and set to zero. This eliminates the effect of noise while retaining the characteristic shapes of the spectra (see Fig. 2). This step was crucial for further data analysis. For most filters, the total intensity removed was 3% or less. For some filters, this percentage was higher, reaching up to 8.2%. This removed intensity is in a part due to noise and artificial background signal of the spectroradiometer varying with wavelength, which is arising from imperfect background subtraction. Other methods for reducing noise while retaining the shape of the transmitted filter irradiance spectra were also tested. This method was chosen as it is universally applicable and independent of the operator.

The light transmitted by the filters depends on the transmission of the filters as well as the spectral irradiance of the light source. Both quantities are the functions of wavelength. The centroid wavelength calculated with (13) considers the actual spectral irradiance used for the measurement. In the absence of knowledge of this spectral irradiance, the centroid wavelength of the filter transmission can be used as an approximation. Our analysis revealed shifts from −6.2 nm to +2.8 nm (see Fig. 3)

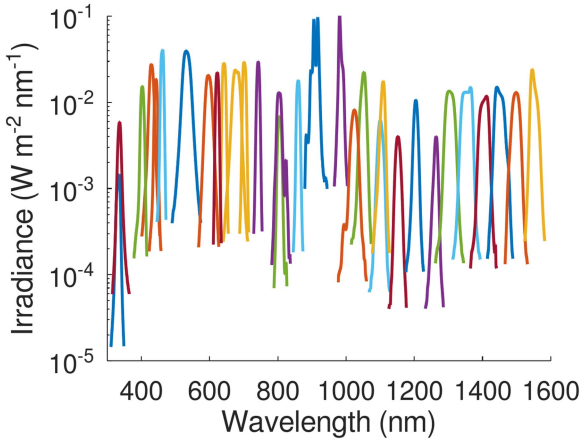

Fig. 1. Transmitted spectral irradiance for selected filters mounted on the Oriel SR setup at ESTI.

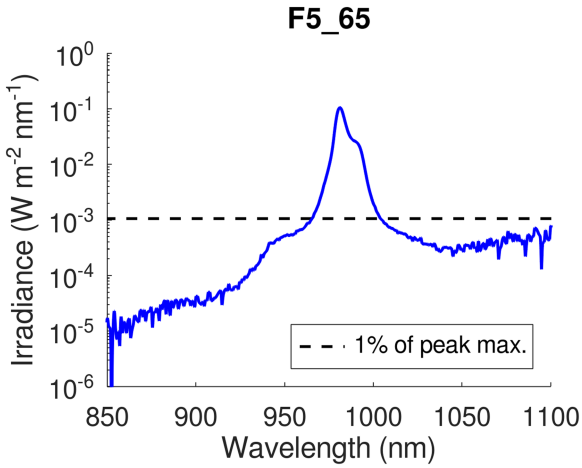

Fig. 2. Cutting off the peak at 1% level for filter F5_65. Note that the vertical scale is logarithmic.

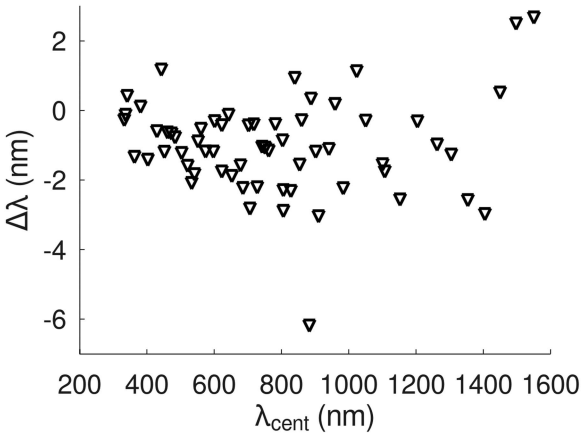

Fig. 3. Comparison of assigned centroid wavelengths (13) against previously used estimate based on the centroid of filter transmission curve.

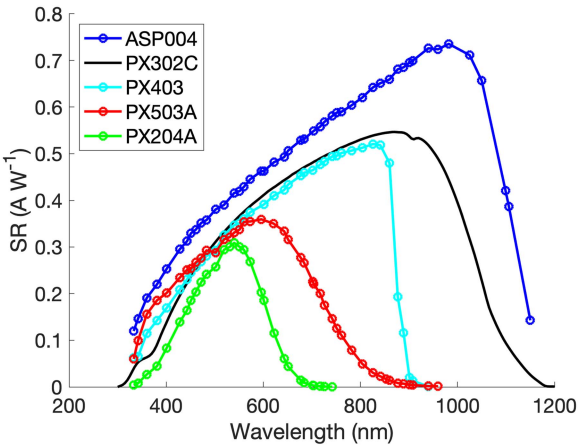

Fig. 4. SR of the four DUTs and the reference cell. The data here are those measured based on (5), i.e., neglecting the bandwidth of the spectral irradiance and assuming perfectly monochromatic irradiance.

between both. This is due to the lamp spectrum having spectral features, such as emission lines. The assignment based on the measured spectral irradiance is more correct as it is this spectral irradiance that generates the current in the PV device, whereas the filter transmission is only an approximation in the absence of knowledge of the actually transmitted spectral irradiance.

B. Spectral Responsivity Measurements

The SR was measured for four different DUTs representing a range of SR shapes: a high-efficiency c-Si cell (ASP004), two filtered c-Si cells (PX204A and PX503A), and a GaAs cell (PX403), all measured against a c-Si reference cell (PX302C). The curves in Fig. 4 are based on (5), assuming perfectly monochromatic light and neglecting the bandwidth of the spectral irradiance transmitted by each filter. The GaAs cell (PX403) was chosen because its SR is very similar to that of CdTe. Both technologies extend over similar wavelength ranges and exhibit sharp transitions from maximum SR to zero SR. GaAs is more stable under irradiation than CdTe cells, which demonstrate

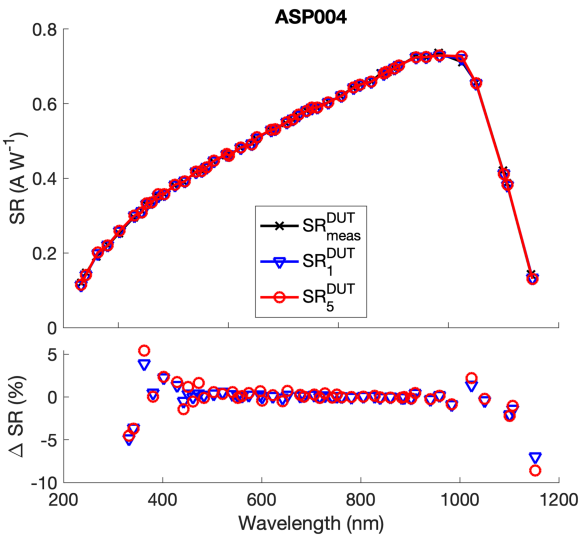

Fig. 5. ASP004: Top: Original SR estimate based on (5) and the SR corrected by the iterative scheme at selected iteration steps; Bottom: Relative difference between iteratively corrected SR and original estimate.

metastability effects due to light soaking. We expect the results for CdTe cells, which are commercially more important in terrestrial PV, to be very similar to those obtained for the GaAs cell.

The SR measurements were made using all filters available in the nonzero SR wavelength range of the DUT. This was done to comprehend how the iterative correction scheme affected results from filters with a variety of spectral irradiance shapes (see Fig. 1). As a general guideline, it is normally sufficient to have one data point every 50 nm. At wavelengths where the SR changes rapidly, one data point every 20 nm is advised. Therefore, not all 64 filters are required to make a standard SR measurement.

C. Iterative Corrections

The iterative correction scheme for SR was applied to all four cells: ASP004 (see Fig. 5), PX403 (see Fig. 6), PX503A (see Fig. 7), and PX204A (see Fig. 8). In all those figures, the original measurement based on (5) (see also Fig. 4) and the corrections at selected iteration steps are shown (top), and additionally the percentage change of the correction (bottom).

In spectral regions, where the SR of DUT and REF is similar, the corrections were small (less than 1%). However, in spectral regions, where two SRs are significantly different, the corrections became substantial.

For ASP004 (see Fig. 5), the corrections range up to 5% for wavelengths below 400 nm and almost 10% above 1100 nm.

Similarly, for PX403 (see Fig. 6), the corrections were significant above 850 nm (where the SR of the DUT rapidly decreases with wavelength, whereas the SR of the REF increases), reaching even 50%.

For PX503A (see Fig. 7), the corrections are more moderate, with up to 5% for the wavelength regions below 400 nm and above 800 nm.

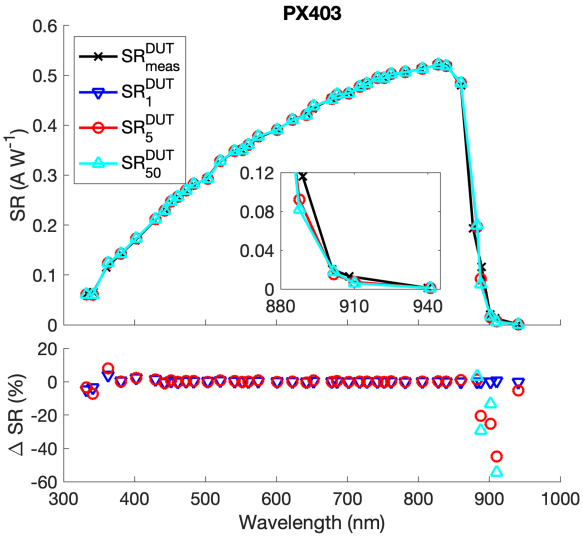

Fig. 6. PX403: Top: Original SR estimate based on (5) and the SR corrected by the iterative scheme at selected iteration steps; Bottom: Relative difference between iteratively corrected SR and original estimate.

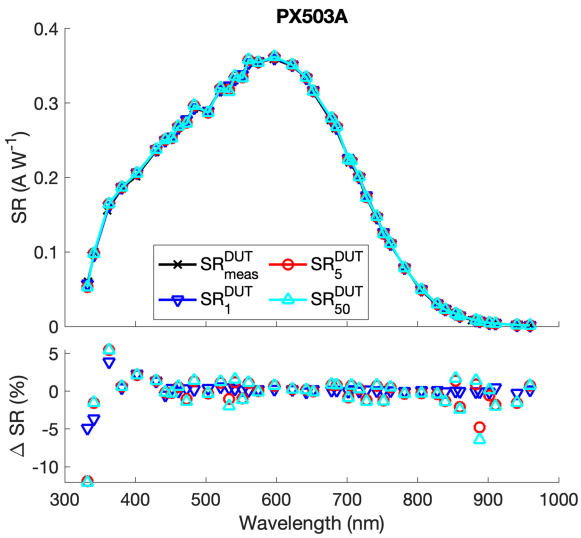

Fig. 7. PX503A: Top: Original SR estimate based on (5) and the SR corrected by the iterative scheme at selected iteration steps; Bottom: Relative difference between iteratively corrected SR and original estimate.

For PX204A (see Fig. 8), the corrections are again more significant, with up to 10% and above for the wavelength regions below 400 nm and above 650 nm.

For all cells, the correction of the SR is most significant in wavelength regions, where the shapes of the SR of DUT and REF are different. This is the case for all four cells for wavelengths below 400 nm. The upper wavelength region depends on the cell, as they have different cutoff wavelengths (see Fig. 4). The correction to SR is nonnegligible with several corrections amounting to 10% and higher.

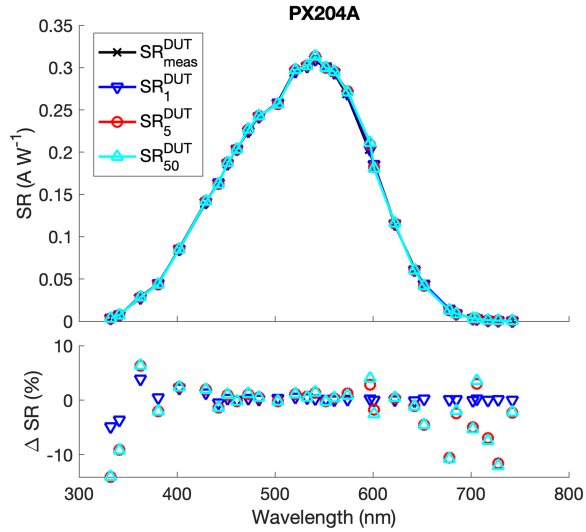

Fig. 8. PX204A: Top: Original SR estimate based on (5) and the SR corrected by the iterative scheme at selected iteration steps; Bottom: Relative difference between iteratively corrected SR and original estimate.

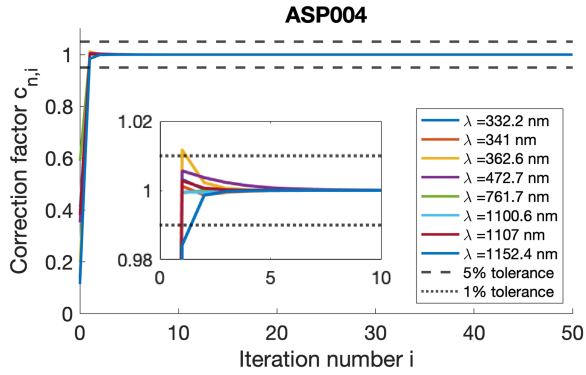

Fig. 9. Correction factor $c_i(\lambda_n)$ versus iteration number i for a selection of filters for ASP004. The filters omitted in the graph converge immediately (two or three iterations), whereas some of the wavelengths shown require a few more iterations.

D. Convergence of Iterative Correction Scheme

The iterative scheme was validated as follows. First, the convergence was tested with all four DUTs. The correction factor converges rapidly enough for practical applications and did not show any artifacts, such as oscillations.

For ASP004 (see Fig. 9), the values for $c_i(\lambda_n)$ converge rapidly toward 1, essentially after two or three iteration steps for almost all wavelengths. The correction factor converged slightly less rapidly for some wavelengths, but full convergence was reached with less than ten iterations in all cases.

For some filters used to measure PX403 (see Fig. 10), the correction is still 2% after five iterations. As the correction of each iteration step is cumulative, this means the following iterations still add significantly to the correction.

The results for PX503A and PX204A (not shown) were very similar to those for ASP004, i.e., full convergence with less than ten iterations.

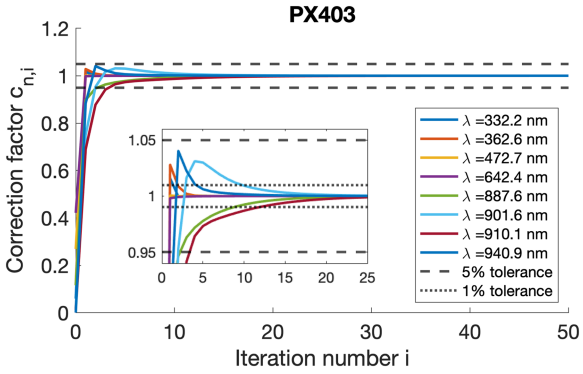

Fig. 10. Correction factor $c_i(\lambda_n)$ versus iteration number i for a selection of filters for PX403. The filters omitted in the graph converge immediately (after two or three iterations), whereas several wavelengths shown require significantly more iterations.

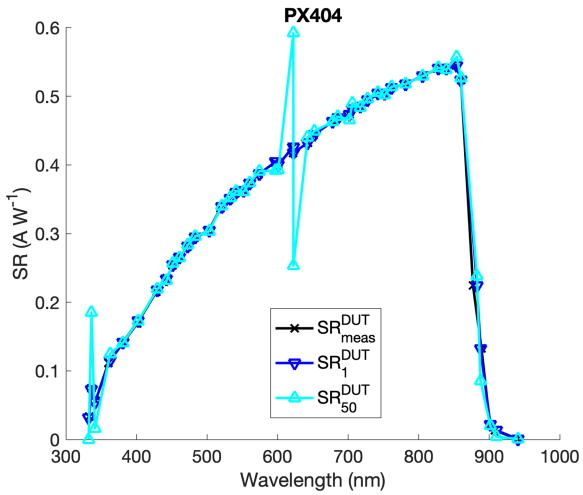

Fig. 11. PX404: Original SR estimate based on (5) and the SR corrected by the iterative scheme at selected iteration steps. The correction generates sharp artifacts around 340 and 620 nm generated due to the noise in measured neighboring data points. The correction has not converged at these wavelengths.

Once implemented, the iterative scheme is not limited by computing time and, therefore, we chose 50 iteration steps (see Figs. 5–8) for all four DUTs. However, even for PX403 and three filters with the slowest convergence (at wavelengths above 850 nm), 25 iterations are fully sufficient (see Fig. 10).

E. Refinement of Iterative Correction Scheme

The SR curves for PV devices are expected to be smooth curves without relevant features. Therefore, some of the smaller features in Figs. 5–8 are attributed to imperfections in the measurement system and noise in the data. This led in some cases to the generation of artifacts in the corrected SR. This became particularly obvious in cases where two filters were used with very similar wavelengths (difference in λ_{cent} less than 3 nm). In these cases, the iterative scheme generated sharp features (see Fig. 11) in the corrected SR and, moreover, convergence was not reached.

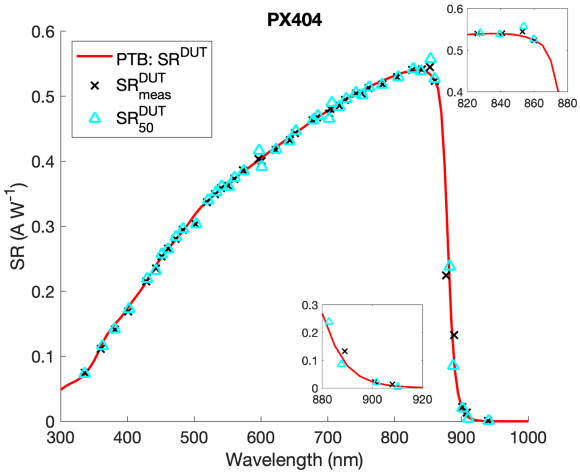

Fig. 12. PX404: Original SR estimate based on (5) and the SR corrected by the iterative scheme after 50 iteration steps compared with the reference measurement from PTB.

The easy solution to this problem is to either not measure two data points at a small interval of wavelength or to eliminate one or the other data point before applying the iterative correction scheme. An averaging of both could be considered but would not be possible in the iterative scheme as the transmitted irradiance $E(\lambda)$ for the averaged data point would be undefined. None of these is satisfactory from a principal point of view in which all measured data should be maintained unless there are clear reasons to declare one as an outlier. While it is actually unlikely to have two measured neighboring data points in practical datasets, here, we tested our method also for this case. We devised a modified correction scheme replacing the piecewise Hermite interpolation, which passes through all data points, with a smoothing spline function, which does not pass through all the data points. Applying the smoothing spline solved the problem of artifacts and divergence, giving an apparently reasonable SR function. However, it was observed that the correction after many iterations was essentially identical to the first iteration. Due to the smoothing spline, the correction for bandwidth that we are trying to achieve was lost. Another aspect is that it is not obvious how to choose the amount of smoothing appropriately. Investigations are still underway to establish whether a smoothing function can be devised in such a way as to avoid artifacts and, at the same time, still correct for filter bandwidth. However, based on our experience, we currently do not recommend this approach.

F. Validation of Method

For final validation, we compared the SR corrected with our iterative scheme to reference data from another laboratory (see Fig. 12). For PX404, a cell very similar to PX403, SR data were available from PTB, Germany, which can be considered as a reference. In general, the results agree well. For some wavelengths (503 nm), the measurement is lower, but this must have other causes than the correction. At other wavelengths (597 nm and 601 nm, and 702 nm and 706 nm), the correction makes the agreement worse. This is due to the artifact introduced

TABLE I
SPECTRAL MMF FOR THE FIVE DUTS AGAINST THE REF UNDER SIMULATED SUNLIGHT FROM THREE DIFFERENT SOLAR SIMULATORS

MMF	Sol Sim	ASP004	PX204A	PX503A	PX403	PX404
SR meas	APOLLO	1.00283	0.99265	1.00457	1.01508	1.01678
	PASAN	1.00007	1.02272	1.01679	1.02233	1.02322
	WACOM	0.99295	1.00790	1.02440	1.04541	1.04604
SR cor	APOLLO	1.00304	0.99241	1.00442	1.01673	1.01841
	PASAN	1.00017	1.02251	1.01657	1.02283	1.02376
	WACOM	0.99311	1.00733	1.02438	1.04596	1.04653
Difference	APOLLO	0.021%	–0.024%	–0.015%	0.163%	0.160%
	PASAN	0.010%	–0.021%	–0.022%	0.049%	0.053%
	WACOM	0.016%	–0.057%	–0.002%	0.053%	0.047%

Calculations were made with measured SR (SR meas) and corrected SR (SR Cor, 50 iterations). Relative difference between both is shown.

by neighboring wavelengths as discussed previously. This will also be partly the reason for the highest point at 854 nm, which is corrected upward due to the neighboring points. On the tailing edge (883 nm and 888 nm), the correction improves the agreement with the reference data (see inset in Fig. 12). It has to be kept in mind that the reference data itself are affected by spectral bandwidth effects.

G. Spectral Mismatch Correction Factor

The SR is most often used for calculating spectral MMF in the electrical performance measurement of PV devices. The MMF was calculated for all five DUTs against the REF for the original SR estimate from the measurement and the iteratively corrected SR (50 iterations). The calculations were made for three solar simulators at ESTI, a large area steady state (APOLLO), a large area pulsed (PASAN), and a smaller area steady state (WACOM) (see Table I). The results show that the MMF varies only weakly with the correction in the SR. This is not surprising as only a few values of the measured SR are significantly affected by the correction. The difference in MMF is irrelevant in most cases and only noticeable in one case (see Table I), namely for the DUT PX403 and PX404 on the APOLLO solar simulator. However, even in this case, it is about three times smaller than the measurement uncertainty of the MMF, which is 0.48%. Nevertheless, this potential additional uncertainty should be considered in the uncertainty budget evaluation if a correction for spectral filter bandwidth is not made to the SR. Adding a fixed uncertainty component for MMF would lead to an overestimation of measurement uncertainty in most cases. Therefore, filter bandwidth correction for SR is recommended also in cases where the main aim of the measurement is the determination of MMF.

IV. CONCLUSION

The iterative correction scheme presented here works without requiring any *a priori* information about the DUT and its SR. A consistent correction to the SR curves of PV devices measured on a filter-based SR system was found. The corrections to the measured SR were more prominent when there are large differences between the SR of the DUT and the reference device. The correction converges after a few iterations. The exact number of iterations depends on the device and filters in question.

It is envisaged that the corrections become more relevant as the filter bandwidth increases. In commercial systems with filter bandwidths of 50 nm or more, the iterative correction scheme should be easily applicable and will have a significant influence on results. This makes the iterative correction scheme important for the SR measurements of PV modules on pulsed solar simulators since these systems typically use filters with larger bandwidths [6]. In the extreme case, where filter bandwidths are approaching or even larger than the SR range of the DUT, information will be lost in the measurement and the correction scheme cannot be successful.

SR curves measured on filter-based systems can, thus, be improved with an iterative correction scheme by considering the bandwidth of the quasi-monochromatic irradiance. This correction scheme has been successfully applied to a filter-based system and can be easily applied to other SR measurement setups if the irradiance of the quasi-monochromatic light transmitted by each filter is known from a measurement with a spectroradiometer. Application to systems using monochromators, LED, or laser light sources is also easily possible but might require slight modifications in the data analysis, such as the treatment of noise in the measured spectral irradiance.

A correction for bandpass filter bandwidth is strongly recommended if the determination of SR is the prime objective of the measurement. In the absence of corrections, a respective component should be added to the measurement uncertainty budget for SR. If the main aim is the calculation of the spectral mismatch correction from the measured SR, as is often the case in PV, the correction for filter bandwidth is, in most cases, negligible and could be omitted. This includes c-Si, which has the majority share in today's commercial PV market.

However, there are cases for which a filter bandwidth correction is beneficial. For example, with the PX403 GaAs cell, a spectral mismatch correction of 0.16% for the APOLLO was observed (see Table I). For a PV calibration laboratory, such as ESTI, which aims and achieves PV performance calibrations at the level of 0.5%, this is not a negligible component. To avoid having to evaluate each case separately, a general implementation of the correction scheme is recommended. The implementation is relatively simple, and for most cases (c-Si), it will neither improve nor deteriorate the data analysis. For a few cases (GaAs and CdTe), it will improve results. An implementation of the correction scheme will be most important for laboratories that characterize cells and modules made from a wide variety of materials.

ACKNOWLEDGMENT

The authors would like to thank their colleagues at ESTI for their support, C. Edmonds thanks D. Pavanello for his guidance on the SR system and the spectroradiometers, B. Mihaylov for discussions related to laboratory work and data analysis, and G. Bardizza for sharing his vast experience with the SR measurement system, and H. Müllejans thanks I. Kröger (PTB, Germany) for the reference data of PX404 and discussion about bandwidth corrections. The views expressed are purely those of the authors and may not in any circumstances be regarded as stating an official position of the European Commission.

REFERENCES

[1] *Photovoltaic Devices—Part 8: Measurement of Spectral Responsivity of a Photovoltaic (PV) Device*, IEC Standard 60904-8, May 2014.

[2] *Photovoltaic Devices—Part 1: Measurement of Photovoltaic Current-Voltage Characteristics*, IEC Standard 60904-1, Sep. 2020.

[3] *Photovoltaic Devices—Part 3: Measurement Principles for Terrestrial Photovoltaic (PV) Solar Devices With Reference Spectral Irradiance Data*, IEC Standard 60904-3, Feb. 2019.

[4] *Photovoltaic Devices—Part 7: Computation of the Spectral Mismatch Correction for Measurements of Photovoltaic Devices*, IEC Standard 60904-7, Aug. 2019.

[5] B. H. Hamadani, J. Roller, B. Dougherty, F. Persaud, and H. W. Yoon, "Absolute spectral responsivity measurements of solar cells by a hybrid optical technique," *Appl. Opt.*, vol. 52, pp. 5184–5193, 2013.

[6] U. Bahrs, W. Zaaiman, M. Mertens, and H. Ossenbrink, "Automatic large area spectral response facility," in *Proc. 14th Eur. Photovolt. Sol. Energy Conf.*, Barcelona, Spain, 1997, pp. 2296–2298.

[7] B. Ebner, G. Agostinelli, and E. Dunlop, "Automated absolute spectral response characterisation for calibration of secondary standards," in *Proc. 16th Eur. Photovolt. Sol. Energy Conf.*, Glasgow, U.K., 2000, pp. 2202–2205.

[8] G. Zaid, S.-N. Park, S. Park, and D.-H. Lee, "Differential spectral responsivity measurement of photovoltaic detectors with a light-emitting-diode-based integrating sphere source," *Appl. Opt.*, vol. 49, no. 35, pp. 6772–6783, 2010.

[9] M. Turek, K. Sporleder, and T. Luka, "Spectral characterization of solar cells and modules using LED-based solar simulators," *Sol. Energy Mater. Sol. Cells*, vol. 194, pp. 142–147, 2019.

[10] P. Kärhä et al., "Measurement setup for differential spectral responsivity of solar cells," *Opt. Rev.*, vol. 27, pp. 195–204, 2020.

[11] S. Winter et al., "Design, realization and uncertainty analysis of a laser-based primary calibration facility for solar cells at PTB," *Measurement*, vol. 51, pp. 457–463, 2014.

[12] E. R. Woolliams, R. Baribeau, A. Bialek, and M. G. Cox, "Spectrometer bandwidth correction for generalized bandpass functions," *Metrologia*, vol. 48, pp. 164–172, 2011.